JOURNAL OF MODERN OPTICS
2003, VOL. 50, NO. 15–17, 2495–2505

Isochoric heating of solid aluminium with picosecond X-ray pulses

G. DYER†, R. SHEPPHERD‡, J. KUBA†, E. FILL§,
A. WOOTTON‡, P. PATEL†, D. PRICE† and T. DITMIRE†

†Department of Physics, University of Texas, Austin, Texas 78712, USA; e-mail: tditmire@physics.utexas.edu

‡Physics and Advanced Technology Directorate, Lawrence Livermore National Laboratory, Livermore, California 94550, USA

§Max-Planck-Institut für Quantenoptik, D-85748 Garching, Germany

(*Received 15 February 2003*)

Abstract. High-energy-density matter in quite unique parameter regimes can be studied using an intense laser pulse to heat isochorically an initially cold solid density target. Such isochoric heating experiments permit study of the properties, such as the equation of state, of heated matter. One of the principal challenges of these experiments is to heat sufficiently thick layers so that they will be inertially confined over times scales sufficient for equilibration, times that are often many picoseconds, even at these high densities. One approach to this problem is to heat a solid target not with the laser pulse directly, which deposits its energy only over a few nanometres, but to heat with penetrating X-rays. In this paper, we present preliminary results where such ultrafast X-ray heating is demonstrated using a short-pulse laser-driven silicon Kα source to heat a layer of solid density aluminium.

1. Introduction

The interactions of high-intensity subpicosecond laser pulses with matter is of great interest for a number of applications, including the production and study of very extreme states of matter. The ability of such an ultrafast laser pulse to deposit energy very quickly leads to the production of very-high-temperature states of matter with a density that of solid density. The study of high-energy-density matter in quite unique parameter regimes is possible if the intense laser pulse can isochorically heat an initially cold solid density target. If temperatures greater than 10 eV are achieved, pressures of 10–1000 Mbar will be present in the solid sample. In principle, such exotic states can be studied if the laser deposits energy much more quickly than the material expands and the material is probed on a time scale that is faster than its inertial confinement [1]. These kinds of isochoric heating experiment are motivated by the fact that a strong understanding of matter in these exotic regimes is not in hand, with even the most sophisticated equation-of-state (EOS) models unable to model this matter accurately [2]. Extending the understanding of EOS in high-energy-density matter is crucial for developing accurate models in a number of fields, including inertial confinement fusion and astrophysics, where such states of hot dense matter are found in many stellar interiors [3].

Journal of Modern Optics ISSN 0950–0340 print/ISSN 1362–3044 online
http://www.tandf.co.uk/journals
DOI: 10.1080/09500340310001598101

Over the last 15 years, since the development of high-energy short-pulse lasers using chirped pulse amplification [4], there have been a number of experimental studies aimed at isochorically heating solid density targets with a femtosecond laser pulse [5–7]. For example, in a recent laser heating experiment, Widmann *et al.* 187 studied aluminium foils of a few hundred ångströms thickness heated by a 100 fs laser pulse to temperatures of about 10 eV . The EOS of this heated aluminium was studied by examining the release of the aluminium slab along an isentrope by interferometric pump–probe techniques. This experiment illustrated that EOS information is possible with short-pulse laser isochoric heating experiments. However, these kinds of experiment have many difficulties which hinder high-quality, well-quantified EOS data. Since the laser deposits its energy in only a skin depth, only a few tens of nanometre of material is heated. Since the inertial confinement time is roughly the thickness of the heated layer divided by the sound speed (often greater than $10^6\,\mathrm{cm\,s^{-1}}$), the laser-heated material releases very rapidly, often on the time scale of the heating laser pulse (about 100 fs). Interpretation of these experiments is further hampered by the fact that the few hundred femtosecond release time of the heated material is comparable with the electron–ion equilibration time (as estimated by the Spitzer [9] theory). The experiments are also complicated by the fact that surface finish of the very thin target often leads to a large uncertainty in the initial density.

Consequently, it is desirable to explore mechanisms of heating larger volumes (ie thicker layers) of material. One promising approaching is to use fast bursts of penetrating radiation, such as fast electrons, protons or X-rays, to heat thicker layers of material than are possible with direct optical heating. For example, fast electrons have been proposed as a means to heat inertial confinement fusion (ICF) targets in the fast ignition concept [10]. Hot electrons accelerated by the interaction of laser pulses with a solid target have been used to heat bulk materials to very high temperatures [11], and ultrashort laser pulses produce bursts of hot electrons on a similar time scale to the pulse itself. Such a large current of electrons travelling closely together through a material follows complex trajectories, making precise energy deposition very difficult to diagnose. Proton heating of solid slabs for high-density EOS measurements have been proposed by Patel and Springer [12]. This approach is attractive as quite high temperatures are possible with the large fluxes of protons possible with short-pulse lasers; however, energy deposition by large proton currents is difficult to diagnose. In contrast, X-rays will follow a straight-line path through space, and their absorption by photoionization is well known, creating the possibility of measuring energy deposition with diagnostics that are well removed from the interaction. If short pulses of X-rays, at appropriate wavelengths, are produced, a well-defined thickness of material will be heated.

We have begun to explore this possibility experimentally. In this paper, we present initial experimental results on the isochoric heating of aluminum with an intense burst of silicon Kα X-rays. In our experiments, we focus an ultrashort laser pulse on to a thin layer of silicon to produce a picosecond pulse of Kα X-rays near 1.8 keV. A specialized etched target design has a thin layer of aluminium held in close proximity to the Kα source while maintaining a precisely measured vacuum gap between the layers. Our initial experiments suggest that the Kα energy absorbed by the aluminium yields several electronvolts per atom. The reflectivity and expansion of the aluminium after heating are probed optically from the side opposite the silicon Kα source layer.

2. Experiment motivation and concept

The description of matter in the pressure and density regime between the realms of high-density plasma physics and high-temperature condensed-matter physics presents a great challenge to researchers. At temperatures of several electron volts and near solid density (10^{-3}–$10\,\mathrm{g\,cm^{-3}}$), constituent atoms are both of high energy and highly correlated. Thus theories that require atom energy to overwhelm correlations, or vice versa, will fail in this regime, known as warm dense matter (WDM). Theoretical treatments of WDM are necessarily very complicated, as they must address such considerations as short- and long-range order, partial ionization and atomic shell structure. Experimental support for theoretical treatments of WDM has been mostly limited to shock experiments [13–15], which access points in density temperature space primarily on the principal shock Hugoniot and, alone, cannot place sufficient constraints to select between various theories. Isochoric heating of a solid or liquid into the WDM regime and observing the release isentrope could provide data in a parameter space distinct from shock experiments on the principal Hugoniot [2].

In an isochoric heating experiment, a solid density sample is heated on a time scale faster than the material expansion time, given roughly as d/c_s if d is the heated layer thickness and c_s is the material sound velocity. Direct optical heating, as used by Widmann *et al.* [8], heats only a few nanometres of material; so the expansion time is fast, about 200 fs (assuming a 10 nm skin depth and a sound speed of about $5 \times 10^6\,\mathrm{cm\,s^{-1}}$ in aluminium heated to about 10 eV). Since the electron–ion equilibration time, even at these high densities, exceeds 1 ps, 200 fs confinement is probably not adequate to realize a proper EOS measurement. This 1–10 ps constraint implies that one needs to heat layers of about 1 μm, yielding confinement times of greater than 10 ps.

Such bulk heating can be achieved with X-ray heating of a layer of material, provided that a suitable high-flux ultrafast source of X-rays can be produced. X-rays with photon energy in the 2–10 keV range will typically exhibit an absorption depth of a few microns in most solid density material (depending, of course, on the atomic number of the absorbing material.) This X-ray isochoric heating technique for studying WDM was first proposed by Lee *et al.* [2]. X-ray heating is attractive because the absorption rate, which will be primarily by photo-ionization in the target, is very well known. The X-rays will couple by photo-ionization, first, into the target's electrons, which will equilibrate among themselves very rapidly (perhaps on the time scale of less than 100 fs at solid density at a temperature of about 10 eV). This will be followed by electron–ion equilibration on a picosecond time scale. Not only are the equilibrium EOS properties of such X-ray heated materials interesting, but also the equilibration dynamics could be studied, if a suitable probe is utilized. X-ray irradiation of solids is also of interest in the study of how X-ray optics will damage in future X-ray free-electron laser machines [16].

One way to produce an intense ultrafast burst of hard X-rays for such an X-ray heating experiment is to use a high-peak-power short-pulse laser to produce Kα radiation on a solid target. It is well known that, when an intense laser irradiates a solid at an intensity greater than $10^{16}\,\mathrm{W\,cm^{-2}}$, fast electrons are produced which enter the cold solid material and produce K-shell holes. These excitations result in a burst of Kα radiation with a pulse duration that can be under 1 ps if produced with an ultrafast laser pulse [17]. Conversion efficiency from laser energy to X-ray energy is about 10^{-4}–10^{-6}, depending on the target material [17,18]. Such

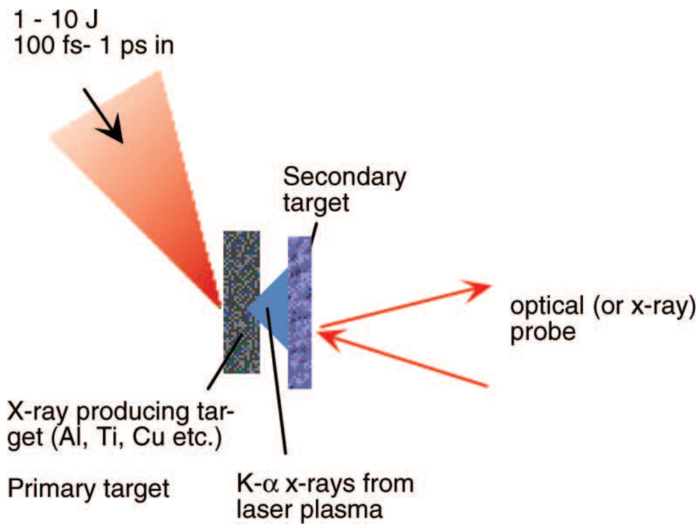

Figure 1. Experimental layout for the laser plasma X-ray heating experiment.

processes produce large amounts of hard X-ray photons in a short pulse and with a narrow bandwidth. The principal disadvantage of using laser-produced Kα X-rays is that they are isotropically emitted and accompanied by other forms of penetrating radiation, namely hot electrons and protons.

To examine X-ray isochoric heating, we have designed an experiment based on the concept illustrated in figure 1. In this approach we hold a sample material in close proximity to a Kα source. The Kα source must be optimized for the production of Kα X-rays over that of other forms of radiation through choice of material composition and dimensions, and tuning of laser parameters [19]. The sample must then be held close to the source in such a way as to isolate it from hot electrons and protons while allowing sufficient amounts of Kα photons to be absorbed.

In our experiment we have chosen to study the heating of solid aluminium. To maximize the X-ray heating for a given X-ray fluence, it is desirable to chose a Kα source with photon energy just above the K absorption edge of the aluminium. This choice of Kα X-rays maximizes absorption. Silicon Kα, with a photon energy of 1.74 keV, is optimum for X-ray heating of aluminium, as illustrated in figure 2. If the silicon X-ray yield is known, we can use the known photo-ionization cross-sections to determine explicitly the deposited energy density in the aluminium layer.

3. Experiment design

Our target design uses a planar geometry (with shape and dimensions illustrated in figure 3). The source and sample are both thin (approximately microns), flat layers of material separated by a vacuum gap several tens of microns wide. A vacuum gap was chosen to stop the free streaming of fast electrons to the secondary aluminium target under study. These electrons are undesirable as they introduce an uncertainty in the deposited energy density. We chose a vacuum gap in lieu of

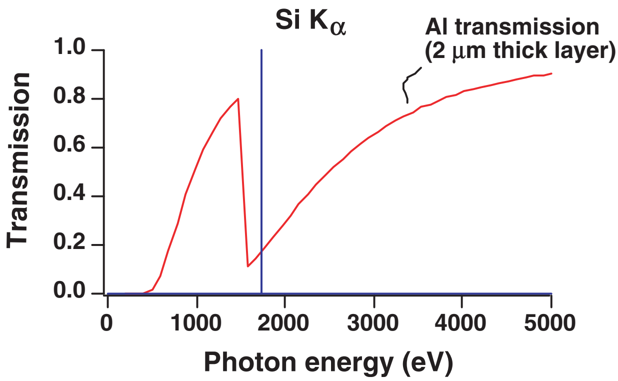

Figure 2. Transmission of an aluminium layer 2 mm thick. The location of silicon Kα radiation is shown, illustrating the fact that this wavelength of X-rays, just above the aluminium K edge is optimal for heating aluminium.

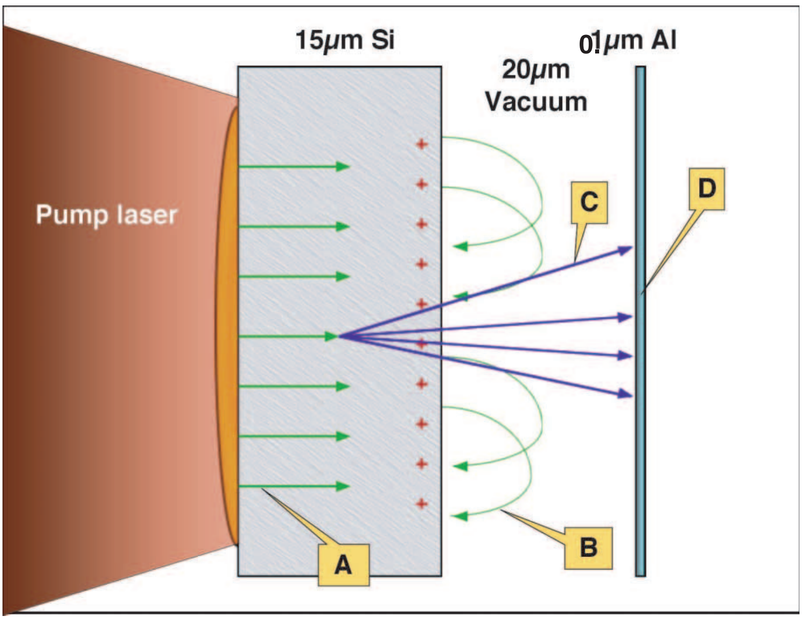

Figure 3. Geometry of Kα heating target: A, hot electrons are accelerated into the silicon source layer, producing K shell holes, which then radiate Kα photons; B, Coulomb forces stop the hot electrons at the back surface of silicon; C, Kα X-rays continue through to the aluminium layer; D, for measurement purposes, it is desirable to achieve mirror flatness on the back side of the aluminium layer.

insulating material because suitable materials were ineffective at stopping the 5–10 keV hot electrons [20, 21]. Instead, we rely on the electron stopping associated with the Coulomb space charge forces involved with large amounts of electrons leaving the source's back surface. The secondary target of aluminium was placed beyond this vacuum gap. The low-Z material aluminium has relatively weak absorption of most hard X-ray energies. Strongest absorption of kiloelectron volt X-rays occurs just past the K-shell ionization edge of the absorbing material. An aluminium layer 1 μm thick absorbs over half the incident silicon Kα protons. However, our first set of experiments were performed with an aluminium layer 0.1 μm thick. This thin layer assured us of uniform energy deposition of the silicon Kα radiation. At the X-ray fluences expected, the temperature of the material was not expected to be greater than 1 eV; so, even with a 100 nm layer, we expect confinement times of longer than 2 ps. To realize the layered target design shown in figure 3, two crystalline silicon wafers 300 μm thick were used. The first wafer was etched down from one side to 15 μm thick within several 'windows' millimetres wide arranged in rows. On the second wafer, spacer groves were etched on one side to achieve the desired 20 μm spacing. Between the grooves, a 500 Å layer of Si_3N_4 is deposited and windows are etched from the other side through to the Si_3N_4. Aluminium is vapour deposited to 0.1 μm on this side, and the two wafers are glued together so that through each target window is silicon 15 μm thick followed by a 20 μm gap, a 500 Å Si_3N_4 layer and then the 0.1 μm aluminium layer. Si_3N_4 absorbs silicon Kα radiation only very weakly and provides support for a mirror-flat aluminium layer. In principle, any combination of source and sample material could be made in this way, as long as a very thin layer of Si_3N_4 is acceptable between them, and as long as both materials can be vapour or otherwise deposited on to a silicon/Si_3N_4 wafer.

X-rays were generated in the silicon layer by irradiating with an 800 nm laser pulse from a titanium:sapphire laser. Shots were performed on the JanUSP laser facility at Lawrence Livermore National Laboratory [22]. JanUSP provides 800 nm, 10 J, 100 fs pulses which can be focused by an off-axis parabola to about 2 μm. However, only modest intensity (less than $10^{17}\,\mathrm{W\,cm^{-2}}$) is needed to produce efficient Kα in silicon; a higher intensity is undesirable as it would produce a large population of very hot electrons (with energy greater than 10 keV) which are inefficient at producing X-rays in the primary layer and are more likely to escape and heat our secondary layer. So, in our experiment the laser was defocused to about 50 μm and stretched to about 1 ps in order to decrease the peak intensity while maintaining high laser energy, and thus optimize for higher Kα output relative to that of electrons and protons.

To derive information on the heated aluminium layer, we optically probe the target with an ultrafast near-infrared pulse. This allows us to measure reflectivity of the material after heating as well as the expansion of the material along its release isentrope. Figure 4 shows the various diagnostics fielded in the first set of experiments. Expansion of the heated aluminium layer is measured with an interferometer. A small piece of the main beam is diverted prior to focusing and steered into a delay leg. This probe beam arrives at the target from −40 ps to 40 ps relative to the arrival of the main pulse and reflects off the aluminium side into a Wollaston prism interferometer [23]. A probe beam imaging system of two achromats and a charge-coupled device (CCD) camera is modified by the insertion of a Wollaston prism just past the focus of the first lens, and a 45° polarizer after the second lens. The Wollaston prism separates the two polarizations of the (45° polarized) probe beam at a slight angle, and the polarizer recombines the polarizations and allows them to interfere at the CCD. The portion of the probe beam interacting with a damaged area can then be interfered with a neighbouring undamaged (flat) region. The fringe spacing is adjusted by changing the prism's position relative to focus of the first lens and also depends on the laser frequency and angle of separation affected the prism.

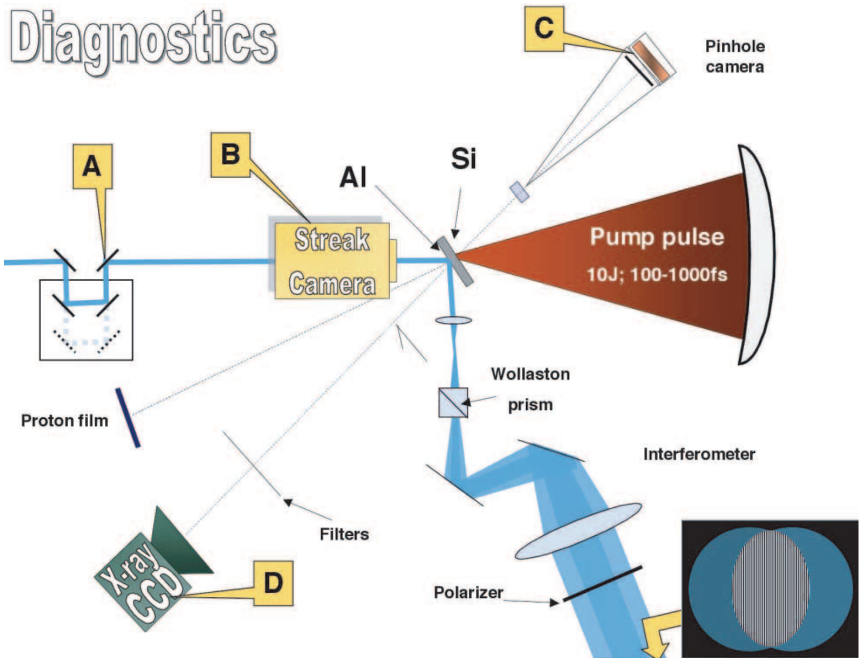

Figure 4. Diagnostics available to our experiment: A, a probe beam is delayed, reflected off the back of the target and entered into a Wollaston prism based interferometer; B, an X-ray streak camera measures the time history of the hard X-ray emission spectrum; C, a pinhole camera with calibrated film can be use to infer a total X-ray fluence near the silicon Kα peak and to infer the source size; D, an X-ray CCD in photon-counting mode can give a spectrally resolved measure of X-ray photon quantities.

Relative timing was varied with a precision of better than 3 fs via a calibrated translation stage. The target was also manipulated by a calibrated translation stage, which allowed for accuracy in the relative timing of probe and main pulses limited only by the pulse width (about 1 ps for this run). To find zero time delay, the target chamber was back-filled with air to 50 Torr and the target is positioned such that the focused main beam just misses its edge. Starting with a large delay, a fringe shift due to field ionization of the gas can be seen until the delay is decreased to a certain point. Since field ionization occurs within a single optical cycle, the transition to zero fringe shift is very precisely identifiable. Combined with the known geometry and well-calibrated positioning of the target, our timing accuracy is as good to within about 100 fs. This probe pulse also yielded target reflectivity.

The other diagnostics measure radiation emitted by the target. An X-ray pinhole camera yielded an absolute measure of X-ray energy radiated at photon energies above about 1 keV, as well as an approximate source size. An X-ray CCD camera, positioned far from the target was used in photon-counting mode to give an absolute spectrum of X-rays passing through the aluminum layer. A knife edge close to the target was used to measure the source size of X-ray radiation. Proton-sensitive film was placed behind the target to measure the energies of the proton beam emitted by the source layer.

4. Results

A lineout from the pinhole camera is shown in figure 5. The X-ray source size was found to be approximately 45 μm, similar to the laser spot size. The integrated X-ray fluence of kiloelectron volt X-rays is measured through use of a densitomiter measurement on the calibrated film. The measured X-ray fluence coming from the short burst of Kα X-rays was about $0.1\,\mathrm{J\,cm^{-2}}$. This X-ray fluence implies an energy deposition of $1\,\mathrm{eV\,atom^{-1}}$ into the 0.1 μm aluminium layer. So we expect after equilibration that the electron and ion temperatures will be somewhat less than 0.5 eV. More detailed calculations of the ionization state at this energy density will be performed to ascertain temperature with greater accuracy.

Interferometer data are presented in figure 6. Expansion of the heated aluminium was inferred from interferometer fringe shifts and is plotted here as a function of time. The material appears to expand initially with a velocity of about $5 \times 10^4\,\mathrm{m\,s^{-1}}$ over a time of about 5 ps. This expansion velocity is faster than we expect, given the level of X-ray heating. For comparison, the expected expansion velocity of a 5 eV and a 100 eV aluminium ideal gas are plotted in figure 6.

The material expansion then seems to accelerate 5 ps after the initial expansion. This apparent increase in temperature at later times may be attributed to fast protons emitted from the back surface of the silicon target. These protons are a well-studied consequence of the arrival of hot electrons on the back surface of a thin target and come from the monlayer of hydrocarbons with usually coat surfaces in a vacuum chamber. Our proton film diagnostics indicated that up to 1 MeV protons were, in fact, emitted by our target, directed normal to the back surface in a narrow cone. These protons seem to have caused expansion that is

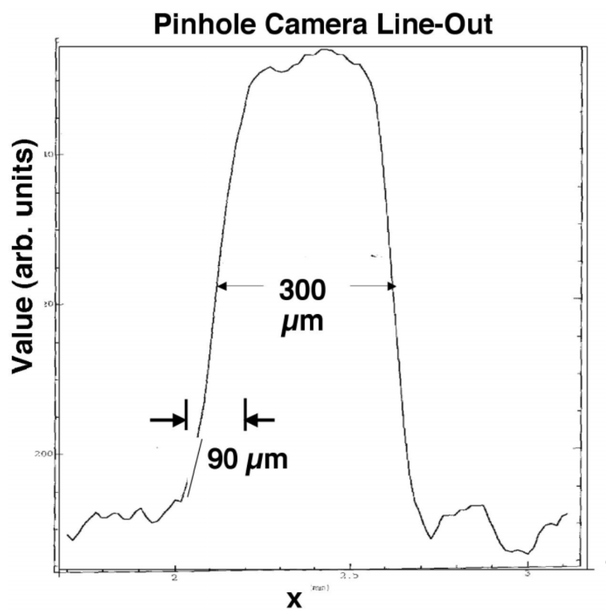

Figure 5. The X-ray source size inferred by the pinhole camera was approximately 45 μm (2 : 1 magnification). The calibrated X-ray film was measured with a densitometer to measure the total X-ray flux at kiloelectron volt photon energies, and hence to infer a Kα X-ray flux on target greater than $1\,\mathrm{J\,cm^{-2}}$.

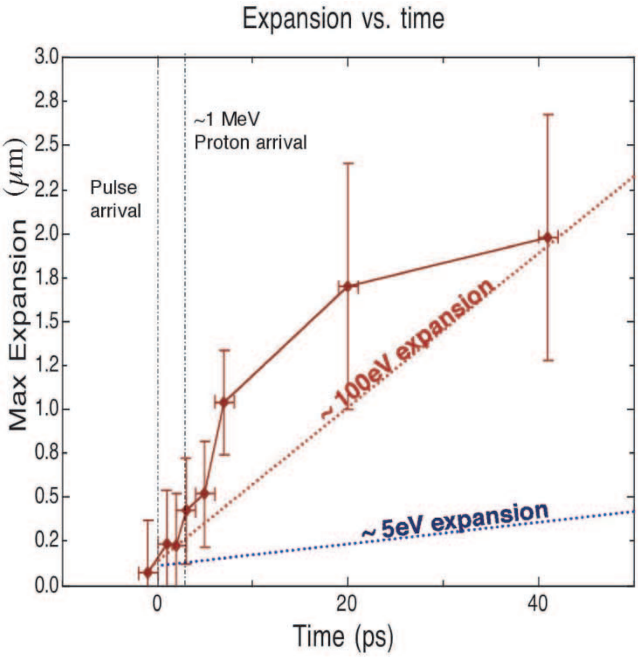

Figure 6. Expansion of the damaged area as a function of time measured by interferometer. The time of arrival for 1 MeV protons originating from the back surface of the silicon layer is drawn. Estimates of expansion speed based on approximate expected sound speed are given for 5 eV and 100 eV temperatures.

much faster than would be expected for heating to approximately 1 eV temperatures. In figure 6, a dotted line indicates the approximate time of arrival for approximately 1 eV protons, to which we attribute the very rapid expansion seen around 5–7 ps. Although heating from protons is a significant issue, these initial experiments indicate that isentropic release data are probably obtainable for a time window less than 5 ps, before the arrival of protons. These data also suggest that we would derive a benefit by using a larger vacuum gap and we intend to quadruple the gap size (to 80 μm) in our next set of experiments where the expansion in the delay range below 5 ps will be more carefully mapped.

We also measure the material reflectivity as a function of time. These data are shown in figure 7. We derived reflectivity changes from the that of cold aluminium by examining the spatial imaged optical probe on the surface and comparing the average pixel value in the centre of the heated region with that in a region just outside in a region of cold aluminium. A transient increase in reflectance is seen a few picoseconds after main pulse arrival. The reflectivity of the heated aluminium is increased by 70% over that of the cold aluminium within 5 ps after heating. We can attribute this to an increased free-electron density caused by a cascade of Auger processes following the initial photo-ionization of Al K shells by the X-rays. The initial arrival of protons also probably contributes to the reflectivity increase. The late time fall off-of reflectivity is likely to be the combined result of electron recombination in the cooling aluminium plasma and the two-dimensional character of the expansion a long time after it has begun.

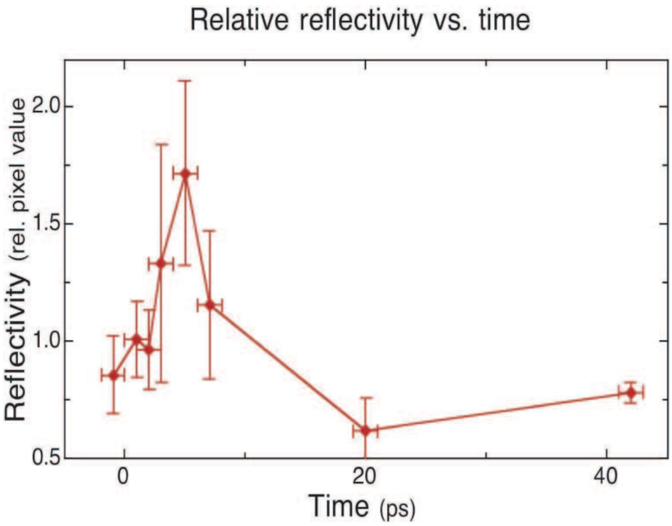

Figure 7. The interferometer produces a second image of the damaged spot in which there was no interference pattern. The relative pixel brightness of a region inside the damaged spot to a fixed region outside the damaged area is plotted as a function of time.

5. Conclusion

These results represent only an initial study of isochoric heating with X-rays. Clearly, more work needs to be carried out to isolate the effects of X-ray heating from the influence of high-energy protons. Revised targets have been designed that better isolate the aluminium layer from the high-energy protons. One type of target increases the vacuum gap to 80 μm, so that there is a much longer delay between the arrival of X-rays and the arrival of energetic protons. Other targets will add to the 20 μm vacuum gap an approximately 25 μm barrier of polypropylene, which is relatively transparent to silicon Kα, but effectively blocks all protons of about 1 MeV or weaker. We believe that with these target improvements we can accurately map the isentropic expansion of the material over the first 10 ps after heating.

In summary, we have presented an experimental design to heat a solid material isochorically to warm temperatures at solid density. Our technique uses the ultrashort and intense burst of Kα X-rays created in intense laser–solid interactions to provide a heating mechanism that is more penetrating than direct optical heating and easier to characterize than hot-electron heating. In our initial experiments, we observed X-ray fluences of about 0.1 J cm^{-2}. These X-ray doses initiated a transient increase in the reflectivity of the aluminium target and started an expansion of the aluminium layer. Hot protons appear to heat the target further about 5 ps after the X-ray initiated expansion starts. Future work is needed to realize the usefulness of this approach, but this technique appears to represent a useful means to study WDM in the laboratory.

References

[1] Murnane, M. M., Kapteyn, H. C., and Falcone, R. W., 1989, *Phys. Rev. Lett.*, **62,** 155.

[2] Lee, R. W., Baldus, H. A., Cauble, R. C., Landen, O. L., Wark, J. S., Ng, A., Rose, S. J., Lewis, C., Riley, D., Gauthier, J.-C., and Audebert, P., 2001, *Plasma-based Studies on 4th Generation Light Sources*, AIP Conference Proceedings, Vol. 581 (New York: Americian Insitute of Physics), pp. 45.

[3] Guillot, T., 1999, *Science*, **286,** 72.

[4] Mourou, G., 1997, *Appl. Phys.* B, **65,** 205.

[5] Forsman, A., Ng, A., Chiu, G., and More, R. M., 1998, *Phys. Rev.* E, **58,** R1248.

[6] Gallant, P., Jiang, Z., Chien, C. Y., Forget, P., Dorchies, F., Kieffer, J. C., Pepin, H., Peyrusse, O., Mourou, G., and Krol, A., 2000, *J. quant. Sptectrosc. Radiat. Transitions,* **65,** 243.

[7] Audebert, P., Shepherd, R., Fournier, K. B., Peyrusse, O., Price, D., Lee, R., Springer, P., Gauthier, J.-C., and Klein, L., 2002, *Phys. Rev. Lett.*, **89,** 265 001.

[8] Widmann, K., Guethlein, G., Foord, M. E., Cauble, R. C., Patterson, F. G., Price, D. F., Rogers, F. J., Springer, P. T., Stewart, R. E., Ng, A., Ao, T., and Forsman, A., 2001, *Phys. Plasmas*, **8,** 3869.

[9] Spitzer, L., 1962, *Physics of Fully Ionized Gases*, (New York: Interscience).

[10] Tabak, M., Hammer, J., Glinsky, M. E., Kruer, W. L., Wilks, S. C., Woodworth, J., Campbell, E. M., Perry, M. D., and Mason, R. J., 1994, *Phys. Plasmas*, **1,** 1626.

[11] Key, M. H., Cable, M. D., Cowan, T. E., Estabrook, E. G., Hammel, B. A., Hatchett, S. P., Henry, E. A., *et al.*, 1998, *Phys. Plasmas*, **5,** 1966.

[12] Patel, P., and Springer, P. T., private communication.

[13] Evans, R., Badger, A. D., Falliès, F., Mahdieh, M., Hall, T. A., Audebert, P., Geindre, J.-P., Gauthier, J.-C., Mysyrowicz, A., Grillon, G., and Antonetti, A., 1991, *Phys. Rev. Lett.*, **77,** 3359.

[14] Volkov, A. P., Voloshin, N. P., Vladimirov, A. S., Nogin, V. N., and Simonenko, V. A., 1980, *Pis'ma Zh. eksp. teor. Fiz.*, **31,** 623 (1980) (Engl. tranl., 1980, *JETP Lett*). **31,** 588.

[15] Rogers, F. J., and Young, D. A., 1997, *Phys. Rev.* E*,* **56,** 5.

[16] *Linac Coherent Light Source Design Study Report,* 1998, Report SLAC-R-521, Stanford Synchrotron Radiation Laboratory, http://www-ssrl.slac.stanford.edu/lcls/design_report/e-toc.html.

[17] Reich, Ch., Gibbon, P., Uschmann, I., and Forster, E., 2000, *Phys. Rev. Lett.*, **84,** 21.

[18] Wharton K. B., Boley, C. D., Komashko, A. M., Rubenchik, A. M., Zweiback, J., Crane, J., Hays, G., Cowan, T. E., and Ditmire, T., 2001, *Phys. Rev.*, E, **64,** 025 401.

[19] Eder, D. C., Pretzler, G., Fill, E., Eidmann, K., and Saemann, A., 1999, *Appl. Phys.* B, **70,** 211.

[20] Koch, J. A., Key, M. H., Freeman, R. R., Hatchett, S. P., Lee, R. W., Pennington, D., Stephens, R. B., and Tabak, M., 2000, *Phys. Rev.* E **65,** 016 410.

[21] Berger, M. J., Coursey, J. S., and Zucker, M. A., 2000, *Stopping-Power and Range Tables for Electrons, Protons, and Helium Ions*, NISTIR 4999, National Institute of Standards and Technology.

[22] Patterson, F. G., Bonlie, J., Rice, D. P., White, B., and Springer, P., 1999, UCRL-JC-134912 Report, Lawrence Livermore National Labouratory, University of California.

[23] Benattar, R., Popovics, C., and Sigel, R., 1979, *Rev. scient. Instrum.*, **50,** 1583.